Hollow Cylinder Radar Cross-Section Pattern Measurement in a Reverberation Chamber

Corentin Charlo, Stéphane Méric, François Sarrazin, Jérôme Sol, Philippe Pouliguen, Elodie Richalot, Philippe Besnier

Hollow Cylinder Radar Cross-Section Pattern Measurement in a Reverberation Chamber

C. Charlo*, S. Méric*, F. Sarrazin*, J. Sol*, P. Pouliguen† E. Richalot‡ and P. Besnier*
*Univ Rennes, INSA Rennes, CNRS, IETR-UMR 6164, F-35000 Rennes, France
Email: corentin.charlo@insa-rennes.fr
†Univ Gustave Eiffel, CNRS, ESYCOM, F-77454 Marne-la-Vallée, France
‡Defense Innovation Agency, French Ministry of Armed Forces, Paris, France

***Abstract*—In this communication, radar cross-section (RCS) measurements of a hollow cylinder are performed within a reverberation chamber and the extracted RCS is compared to the one obtained through anechoic chamber measurements and CST studio simulations. The satisfying agreement between the three approaches shows accurate RCS characterization can be obtained in RC.**

***Index Terms*—Radar Cross-Section, Reverberation Chamber, Anechoic Chamber, Measurements.**

I. Introduction

Nowadays, reverberation chamber (RC) measurements are more and more used as a complement to anechoic chamber measurements. Some articles and books present various applications of characterization within RCs [1]–[3], including antenna radiation pattern measurement [4]–[6] and target radar cross-section (RCS) characterization [7], [8].

Radar cross-section describes the behaviour of a target when exposed to an electromagnetic field. Its characterization is nowadays important for many applications (electromagnetic compatibility tests, antenna characterization, over-the-air testing of wireless devices). RCS is usually measured in anechoic chambers (ACs) to extract the line-of-sight contribution and limit the multipath contributions. However, it is possible to extract the RCS of a target through measurement in an RC with an appropriate method. Several different methods exist to extract the RCS of a target. A post-processing with a time-gating method has been proposed for RCS extraction in RC [9], where the time-gating is applied to the time-domain signal obtained through an inverse Fourier transform. This method used to isolate the response of the target corresponds to the classical approach used in an AC. Another method could be used to estimate the RCS [10], based on the estimation of the Ricean K-factor [11], that permits to extract the line-of-sight signal between the target and the antennas. The RCS could then be extracted but the dynamic range of this appraoch is limited. In this article, the RCS is estimated with a different method. A sinusoidal regression is applied on the difference of the S-parameters measured in the loaded room with the target and the empty room [7], [8], [12]. The extraction method has been improved as described in [13].

This article is organized as follows. Section II explains briefly the principle of RCS measurement in RCs. Then, section III presents the RCS measurement in AC with the one extracted from CST Studio Suite simulation; these results will be considered as references in the following comparison. The Section IV presents the measurement setup in RC. In Section V, the RCS measurement results in RC is compared to the references. The last section concludes.

II. Theory of RCS measurement in RCs

The theoretical development of the method is detailed in [7], [8], [12] and is summarized in this section. To extract the RCS, the difference of the transmission parameters between both antennas measured in the empty RC ($S_{12}(f_0)$) and the target-loaded RC ($S_{12}^T(f_0)$) is computed.

$$S_{12}^{\mathrm{T}}(f_0) - S_{12}(f_0) = B(f_0) + \sqrt{\sigma^{\mathrm{T}}(f_0)}A(f_0)\exp\frac{-\mathrm{j}2\pi f_0 2R}{c}\exp(\mathrm{j}\phi_0) \quad (1)$$

$B(f_0)$ depends on the antenna properties and on the difference of two random variables representing the RC transfer function with and without the target. The second term corresponding to the radar echo is proportional to the target RCS square root. Using a sinusoidal regression, the amplitude of this line-of-sight path between the antennas and the target is estimated and the RCS is then computed.

III. RCS references

Our references correspond to the RCS measured in an AC and the one simulated using CST Studio Suite.

A. Anechoic Chamber

The AC used is the CHEOPS test facility from the French Ministry of Defense (DGA/MI). This chamber is used for small missile RCS measurements as well as antenna characterizations. The dimensions of the Faraday cage are 25 m long, 12 m high, and 12 m large. It is totally covered with pyramidal radar absorbing materials. This anechoic chamber benefits from a huge precision with a sensibility of -70 dBm^2 and a dynamic range of 70 dB. The target is placed on a mast that can rotate in the azimuth plane between $0°$ and $360°$ with a step of $0.001°$. The RCS measurement in this AC is made in three steps. The first step consists of the measurement of the S parameters of the empty room. This measurement permits to estimate the electromagnetic echo

that is not absorbed by the absorbing materials as well as the coupling between the antennas. Then, in a second step, the S parameters are measured in the room charged with a reference target. This reference target is usually a metallic plate. Finally, the last step is a measurement of the S parameters with the target to characterize, that is the hollow cylinder in our case. These three measurements permit to extract the target RCS. For that purpose, two S parameter differences are computed. The first difference is calculated between the empty room and the room charged with the reference target whereas the second difference is calculted between the empty room and the one with the target to characterize. These differences permit to extract the target response from the AC contribution. The knowledge of the response of the reference target along with the theoretical expression of its RCS σ_{ref} makes possible to apply a correction on the measurement results with the target under test using the Eq. (2) to estimate the target RCS σ_{target}.

$$\sigma_{target} = \left| \frac{S_{12}^{target} - S_{12}^{empty}}{S_{12}^{ref} - S_{12}^{empty}} \right|^2 \sigma_{ref} \qquad (2)$$

B. CST Studio Suite

The RCS module of CST Studio Suite is used to compute the target RCS. A plane wave excitation is considered that corresponds to a source in the far-field area; this condition is respected in the AC setup but not in the RC one. The target is considered as made of perfect electric conductor and placed in vacuum. The simulation is performed at 9.2 GHz using the frequency solver, and the accuracy is fixed to -40 dB. The RCS is computed over an azimuth range between $0°$ and $+90°$ with a $1°$ step.

IV. Measurement Set-up in RC

Measurements are performed in the RC of the IETR in VV polarization. The dimensions of the RC are $2.9 \times 3.7 \times 8.7$ m^3. Two antennas are used in a quasi-monostatic configuration. In fact, the distance between the antennas and the target $R' = 4.6$ m is much larger than the distance between the two antennas (0.3 m). The antennas are oriented towards the target. It has been verified that the coupling between the antennas does not affect the measurement results [12]. The measurement set-up is detailled in Fig. 1a. The target, described in Fig. 1b, is a metallic cylinder with a shallow excavation compared to its diameter. The height and the diameter of this cylinder are of 30 cm. The shallow excavation at the middle of the cylinder has a section of 15×7.5 cm^2 and a depth of 2 cm. This depth is close to the wavelength $\lambda = \frac{c}{f} \approx 3.3$ cm.

V. Measurement Results

In this section , the target is illuminated in VV polarization. The measurement method detailed in [13] is followed. The post-processing method is composed of two steps. The first step consists of estimating the distance between the antennas and the target while considering the measurement results on a large frequency band of 4 GHz. Using this estimated distance,

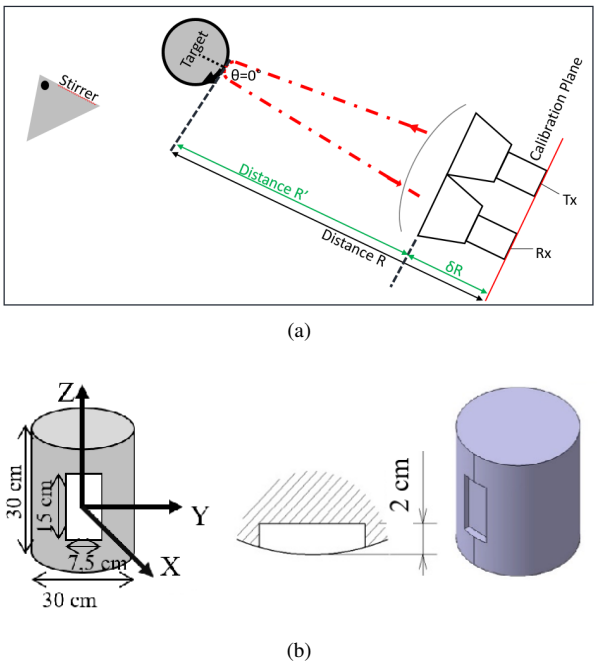

Fig. 1: Schematic description with distance definitions of the test setup with a cylindrical target in the RC (a) and Description of the measured metallic cylinder with the shallow excavation (b).

the amplitude of the radar echo is then extracted from a restricted bandwidth of 0.9 GHz. As shown in Section II, this amplitude is proportionnal to the RCS square root. The result correction based on Eq. (2) is applied with a cylindric target without excavation as the reference target; indeed, the measurement of our target at the angle where the hole is at the position opposed to the antennas is used. Then the RCS of the hollow cylinder target is computed.

Fig. 2 presents the angular variation of the estimated distance between the antennas and the target, this distance being then used to estimate the target RCS. This distance is greater than the geometrical distance between the target and the antennas R' as the calibration planes are not situated at the antenna openings. We notice that the shallow excavation is observed with a higher distance between $\theta = -14°$ and $\theta = +14°$, whereas the distance is more stable on the other azimuth positions.

Fig. 3 shows a comparison of the RCS extracted from RC measurements with the ones obtained through classical measurements in an AC and from simulations. The similarity between the three curves shows that the RCS estimation from RC measurements can lead to reliable results. In particular the RCS measured in RC is close to the reference ones for azimuth positions between $20°$ and $60°$. The local minima and maxima are at the same positions but there are some differences between the estimated amplitudes, in particular around $\theta = 0°$. Part of the remaining measurement errors may be attributed to alignment issues in the RC.

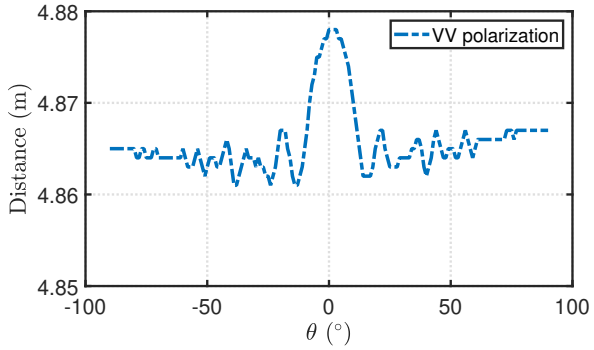

Fig. 2: Estimation of the distance between the target and the antennas as a function of the azimuth angle θ varying from $\theta = -90°$ to $\theta = -+90°$.

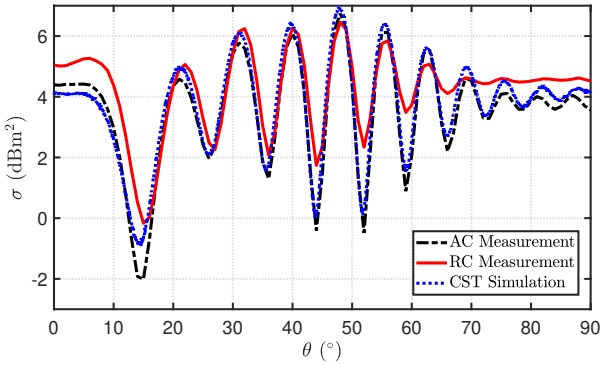

Fig. 3: Comparaison of RCS measurements in RC and AC with simulated one using CST Studio Suite in VV polarization.

VI. Conclusion

This communication highlights that the RCS measurement in an RC is close to the RCS measurement in an AC, so that this characterization method could be considered as an alternative. We have shown that is is possible to estimate the RCS pattern of a complex target with a good accuracy with regard to the reference result obtained in AC or the simulated one. Thus the accuracy and the reliability of the presented method has been demonstrated.

However, our RCS extraction method relies on the hypothesis of a target acting as a point-like target. Therefore our future works will focus on more complex multiple point-like targets. This will require developping a new signal processing approach.

ACKNOWLEDGEMENT

This work is supported by AID/DGA, France. It is also supported in part by the European Union through the European Regional Development Fund, in part by the Ministry of Higher Education and Research, in part by the Région Bretagne, and in part by the Département d'Ille et Vilaine through the CPER Project SOPHIE/STIC & Ondes.

References

[1] P. Corona, G. Latmiral, E. Paolini and L. Piccioli, "Use of a Reverberating Enclosure for Measurements of Radiated Power in the Microwave Range," in IEEE Transactions on Electromagnetic Compatibility, vol. EMC-18, no. 2, pp. 54-59, May 1976,

[2] P. Besnier, and B. Démoulin. "Electromagnetic reverberation chambers." John Wiley & Sons, 2013.

[3] G. Andrieu, ed. "Electromagnetic Reverberation Chambers: Recent advances and innovative applications." IET Digital Library, 2020.

[4] M. Á. García-Fernández, D. Carsenat and C. Decroze, "Antenna Radiation Pattern Measurements in Reverberation Chamber Using Plane Wave Decomposition," in IEEE Transactions on Antennas and Propagation, vol. 61, no. 10, pp. 5000-5007, Oct. 2013.

[5] M. Á. García-Fernández, D. Carsenat and C. Decroze, "Antenna Gain and Radiation Pattern Measurements in Reverberation Chamber Using Doppler Effect," in IEEE Transactions on Antennas and Propagation, vol. 62, no. 10, pp. 5389-5394, Oct. 2014.

[6] A. Soltane, G. Andrieu, E. Perrin, C. Decroze and A. Reineix, "Antenna Radiation Pattern Measurement in a Reverberating Enclosure Using the Time-Gating Technique," in IEEE Antennas and Wireless Propagation Letters, vol. 19, no. 1, pp. 183-187, Jan. 2020.

[7] P. Besnier, J. Sol, and S. Méric, "Estimating radar cross-section of canonical targets in reverberation chamber," in 2017 Int. Symp. on Electromagn. Compat. - EMC EUROPE, 2017, pp. 1-5.

[8] A. Reis, F. Sarrazin, E. Richalot, S. Méric, J. Sol, P. Pouliguen and P. Besnier, "Radar Cross Section Pattern Measurements in a Mode-Stirred Reverberation Chamber: Theory and Experiments", in IEEE Transactions on Antennas and Propagation, vol. 69, no. 9, pp. 5942–5952.

[9] A. Soltane, G. Andrieu and A. Reineix, "Monostatic Radar Cross-Section Estimation of Canonical Targets in Reverberating Room Using Time-Gating Technique," 2018 International Symposium on Electromagnetic Compatibility (EMC EUROPE), Amsterdam, Netherlands, 2018, pp. 355-359.

[10] A. Sorrentino, G. Ferrara, M. Migliaccio and S. Cappa. (2018). "Measurements of Backscattering from a Dihedral Corner in a Reverberating Chamber," Applied Computational Electromagnetics Society Newsletter. 33. 91-94.

[11] C. Lemoine, E. Amador and P. Besnier, "On the K-Factor Estimation for Rician Channel Simulated in Reverberation Chamber," in IEEE Transactions on Antennas and Propagation, vol. 59, no. 3, pp. 1003-1012, March 2011, doi: 10.1109/TAP.2010.2103003.

[12] C. Charlo., P. Besnier, and S. Méric, "Quasi-monostatic Radar Cross-Section Measurement in Reverberation Chamber," in 2021 18th European Radar Conference (EuRAD), 2022, pp. 94-97.

[13] C. Charlo, S. Méric, F. Sarrazin, E. Richalot, J. Sol, P. Besnier, "Advanced Analysis of Radar Cross-section Measurements in Reverberation Environments," PIER Journal to be published.